

# Effect of the Extent of Cure on the Modulus, Glass Transition, Water Absorption, and Density of an Amine-Cured Epoxy

JOHN B. ENNS\* and JOHN K. GILLHAM, *Polymer Materials Program, Department of Chemical Engineering, Princeton University, Princeton, New Jersey 08544*

## Synopsis

The modulus, density, glass transition temperature ( $T_g$ ), and water absorption characteristics of an amine-cured resin [diglycidyl ether of bisphenol A (Epon 828)/diaminodiphenyl sulfone (DDS)] were studied as a function of extent of cure. The glass transition is a function of the extent of cure and reaches a maximum temperature,  $T_{g\infty}$ , when it is completely cured; specimens with different extents of cure were formed by isothermal cure below  $T_{g\infty}$  for different times. After slowly cooling, the density at each extent of cure was obtained at room temperature. Moisture absorption was monitored gravimetrically at 25°C for 2 months at several humidity levels. The room temperature density and modulus decreased with increasing extent of conversion whereas the glass transition temperature and equilibrium water absorption increased. The equilibrium water absorption increased linearly with relative humidity, and the absorptivity increased linearly with specific volume. An interpretation of these anomalous results is made in terms of the nonequilibrium nature of the glassy state. The glass transition temperature increases as the extent of cure increases resulting in a material that is further from equilibrium at room temperature and therefore has more free volume and a greater propensity to absorb water.

## INTRODUCTION

The curing phenomena of a thermosetting epoxy resin can be understood in terms of a time-temperature-transformation (TTT) cure diagram<sup>1</sup> in which the times to gelation and vitrification are plotted versus the isothermal cure temperature. As can be seen in Figure 1, the S-shaped vitrification curve and the gelation curve divide the time-temperature plot into four distinct states of matter: liquid, gelled rubber, ungelled glass, and gelled glass.  $T_{g0}$  is the glass transition temperature of the unreacted resin mixture,  $T_{g\infty}$  is the glass transition temperature of the fully cured resin, and  $_{gel}T_g$  is the glass transition temperature of the resin at its gel point.

The times to gelation and vitrification can be determined from the loss peaks of an isothermal dynamic mechanical spectrum obtained using the torsional braid analysis (TBA) technique.<sup>1,2</sup> At cure temperatures sufficiently below  $T_{g\infty}$ , the reaction will not go to completion because, as the viscosity increases (a result of the increasing molecular weight), the reaction becomes diffusion controlled and eventually is quenched as the material vitrifies.<sup>3</sup> The extent of conversion attained when the reaction is quenched increases as the cure temperature is raised, as evidenced by a corresponding increase in the glass transition temperature.

In addition to the increase in the glass transition temperature, other parameters can be monitored as a function of the extent of cure in an attempt to un-

\* Present address: Bell Laboratories, Whippany, NJ 07981.

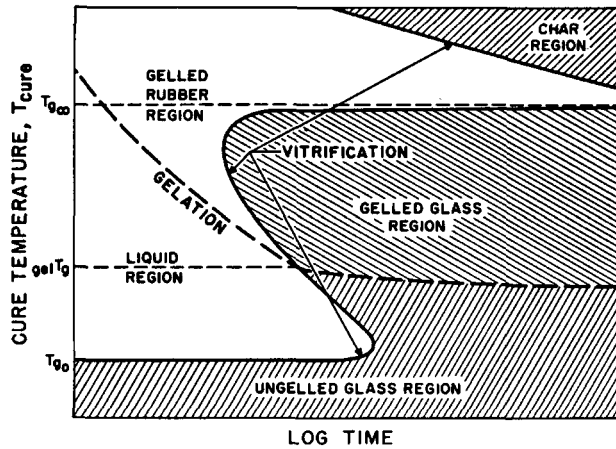


Fig. 1. Time-temperature-transformation (TTT) cure diagram (schematic).

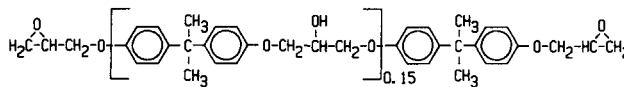
understand the changes that occur during cure. These include the shear modulus (of a film which can be measured with a torsion pendulum), the room temperature density, and the room temperature equilibrium water absorption.

In this paper, the above-mentioned techniques, as well as gel fraction experiments to identify the gel time in the dynamic mechanical spectra,<sup>4</sup> have been used to monitor the changes in physical properties that occur during cure. A preliminary report from this laboratory has been published.<sup>5</sup>

## EXPERIMENTAL

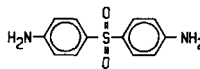
**Materials.** A stoichiometric mixture of the diglycidyl ether of bisphenol A (Epon 828; Shell) and 4,4'-diaminodiphenyl sulfone (DDS; Aldrich) was prepared for the investigation (see Fig. 2). For the TBA experiments each of the components was dissolved in methylethylketone (MEK) before mixing. For the other experiments the amine was added after the epoxy had been heated to

EPOXY: Diglycidyl Ether of Bisphenol A (EPON 828)



+

AMINE: 4,4'-Diaminodiphenyl Sulfone (DDS)



↓

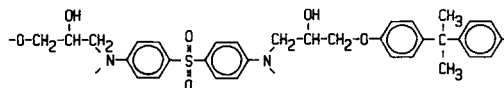


Fig. 2. Chemical structures of reactants and crosslinking site.

130°C; the mixture was stirred until the amine dissolved in the epoxy (<5 min). Equal amounts (by weight) of the neat resin were poured into aluminum foil-lined aluminum molds (2 in.  $\times$  0.5 in.  $\times$  0.0625 in.), degassed in a vacuum oven ( $\sim$ 1 Torr) at 80°C for 20 min (until the bubbles disappeared), and placed in a heated oven (purged with nitrogen) at 175°C to cure. After curing for specified times (50, 100, 180, and 600 min), the specimens were allowed to cool slowly to room temperature in the oven and then were placed in a dessicator. The cured specimens were clear, indicating that the mixture had not phase-separated during the process.

**Torsional Braid Analysis (TBA).** Supported TBA specimens were made by dipping a multifilamented glass braid into a resin/MEK solution (20% resin). They were then mounted in the specimen chamber in a helium atmosphere at the temperature of cure, and their modulus and logarithmic decrement were monitored by an automated apparatus<sup>2</sup> until the reaction was either complete or quenched, as indicated by a leveling off of the modulus. Typically, two peaks in logarithmic decrement were observed during cure, identified as a liquid-to-rubber transformation (gelation) and a rubber-to-glass transformation (vitrification), respectively. Representative spectra are shown in Figure 3, and the

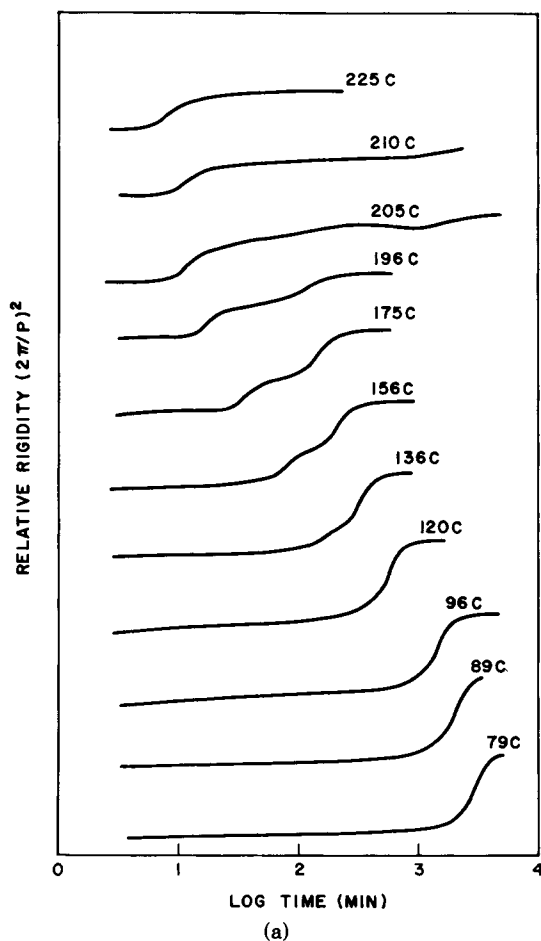


Fig. 3. Isothermal TBA spectra: (a) relative rigidity; (b) logarithmic decrement.

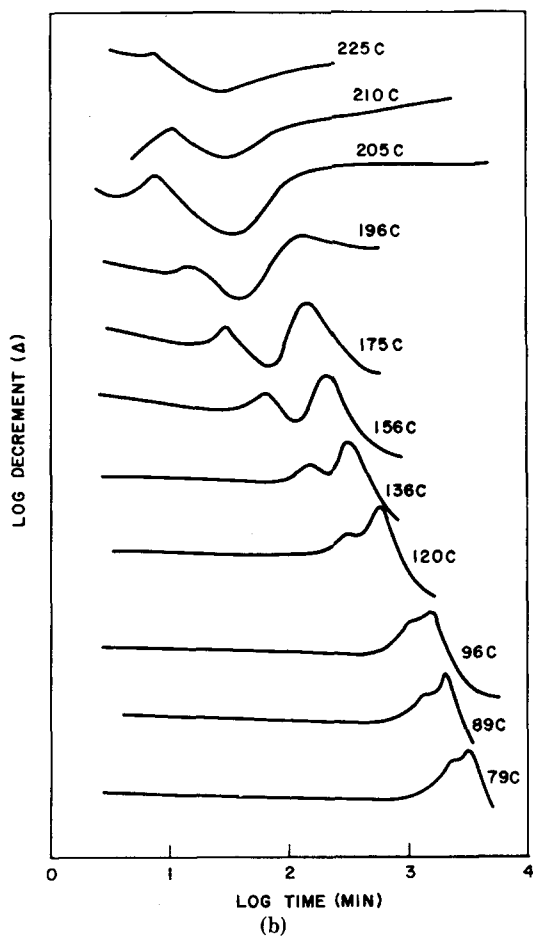


Fig. 3 (Continued from the previous page.)

times to these events are tabulated in Table I. Thermomechanical spectra were then obtained on cooling to  $-190^{\circ}\text{C}$  (at  $1.5^{\circ}\text{C}/\text{min}$ ) and heating to  $250^{\circ}\text{C}$  (at the same rate). Since the resin can be fully cured by heating the partially cured resin

TABLE I  
Summary of TBA Data

$T_{\text{cure}} (^{\circ}\text{C})$	$t_{\text{liquid-to-rubber}} (\text{min})$	$t_{\text{vit}} (\text{min})$	$T_{\text{sec}} (^{\circ}\text{C})$	$T_{\text{sec}\infty} (^{\circ}\text{C})$	$T_g (^{\circ}\text{C})$	$T_{g\infty} (^{\circ}\text{C})$
225	8			-35	215	215
210	11	>2400		-41	204	
205	12	130		-40		208
196	15	135		-42	205	205
175	31	144	-41	-30	203	210
156	67	215	-45	-43	181	211
136	151	337	-47	-35	162	206
120	333	569	-58	-38	145	204
96	1285	1498	-74	-39	124	210
89	1490	1996	-79	-36	108	207
79	2357	3083		-39	97	206

above  $T_{g\infty}$  ( $= 210^\circ\text{C}$ ), a subsequent scan from  $250^\circ\text{C}$  to  $-190^\circ\text{C}$  was considered to provide the spectrum of the fully cured resin. Two major relaxations are observed in these spectra: the glass transition ( $T_g$ ) and a secondary subglass transition ( $T_{\text{sec}}$ ) related to the motion of the  $-\text{CH}_2-\text{CH}(\text{OH})-\text{CH}_2-\text{O}-$  group in the epoxy.<sup>6</sup> The values of  $T_{\text{sec}}$ ,  $T_{\text{sec}\infty}$ ,  $T_g$ , and  $T_{g\infty}$  obtained from these scans are tabulated in Table I and plotted in Figure 4.  $T_{\text{sec}}$  and  $T_g$  increase with increasing extent of cure to approach  $T_{\text{sec}\infty}$  and  $T_{g\infty}$ , respectively. It is noted that the glass transition temperature after prolonged isothermal cure at temperatures below  $T_{g\infty}$  is higher than the temperature of cure.<sup>4,7</sup>

In order to monitor the increase in the glass transition during isothermal cure at  $175^\circ\text{C}$ , the curve was interrupted at selected times (using separate samples), and a temperature scan made to determine the glass transition temperature. The spectra of the partially cured specimens and subsequently fully cured specimens are shown in Figure 5; the glass transition temperatures vs. time of cure are shown in Figure 6. Note that 600 min at  $175^\circ\text{C}$  was insufficient to fully cure the resin.

**Torsion Pendulum.** A film of Epon 828/DDS, prepared as described above by partially curing at  $175^\circ\text{C}$  for 100 min, was machined to dimensions of  $4.70 \times 0.60 \times 0.063$  cm and mounted in a calibrated torsion pendulum<sup>2</sup>. Thermomechanical spectra displaying quantitative values of the elastic shear modulus ( $G'$ ) and logarithmic decrement ( $\Delta$ ) of the partially cured specimen were obtained on cooling to  $-190^\circ\text{C}$  (not shown in Fig. 7) and subsequent heating (Fig. 7) to  $250^\circ\text{C}$ . The spectrum of the fully cured film was then obtained on cooling to  $-190^\circ\text{C}$  (Fig. 7).

**Gel Fraction.** Two independent experiments were conducted to estimate the gel times of the resin at various temperatures; in one the reaction was conducted in an air atmosphere, whereas in the other a helium atmosphere was used. In the former case, open test tubes containing approximately 5 mL of resin were placed in a heated oil bath. The test tubes were removed at selected intervals,

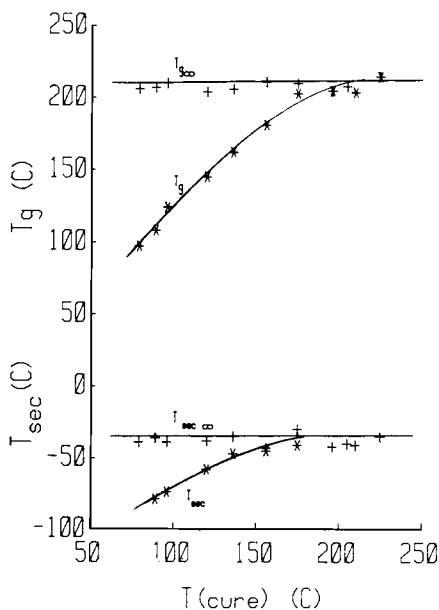


Fig. 4.  $T_{\text{sec}}$  and  $T_g$  vs. cure temperature; (\*) as cured; (+) postcured.

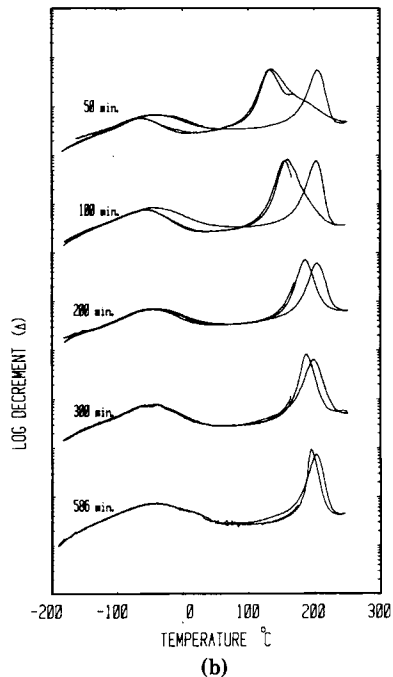
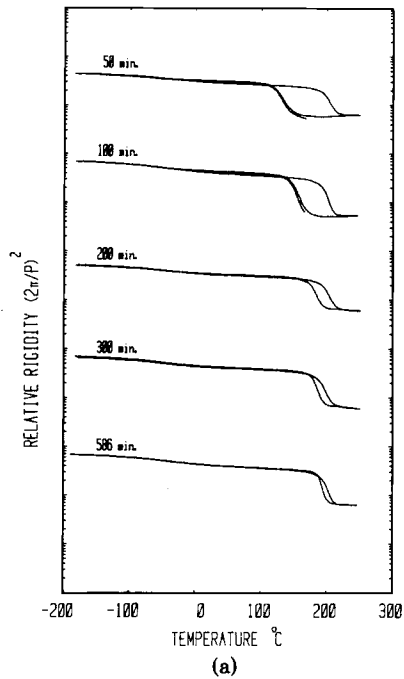


Fig. 5. TBA spectra after curing at 175°C for various times. 175°C to -190°C to 250°C to -190°C at 1.5°C/min. (a) Relative rigidity; (b) logarithmic decrement.

cooled, and the soluble portion extracted with MEK for 48 h. The insoluble portion (gel) was then dried, weighed, and compared with the initial weight (before extraction) to give a gel fraction. This procedure was carried out with

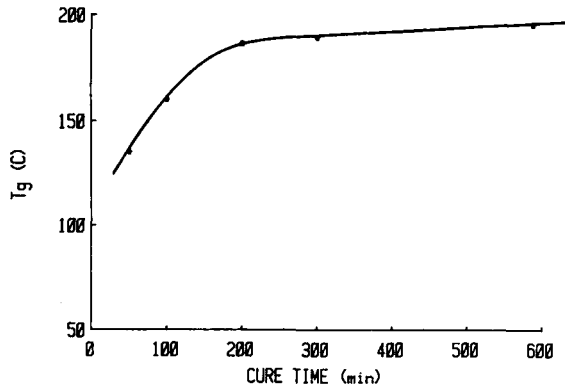


Fig. 6.  $T_g$  vs. cure time at 175°C.

11 or more samples at each of 10 cure temperatures ranging from 102°C to 202°C; the data are shown in Figures 8(a) and 8(b).

In the second experiment, 1–2 mL of resin were placed in ampules, degassed for 20 min (until the bubbles disappeared) at 1 Torr, sealed in a helium atmosphere, and placed in a heated oil bath held at a fixed temperature. The ampules were removed at selected intervals, quenched in liquid nitrogen, broken, and the soluble portion extracted with MEK for 3 h using a Soxhlet extraction column with coarse thimbles. The insoluble portion (gel) was then dried, weighed, and compared with the initial weight (before extraction) to give a gel fraction. This procedure was carried out at each of seven cure temperatures ranging from 132°C to 184°C; the data are shown in Figure 8(c). The gel points for both experiments,

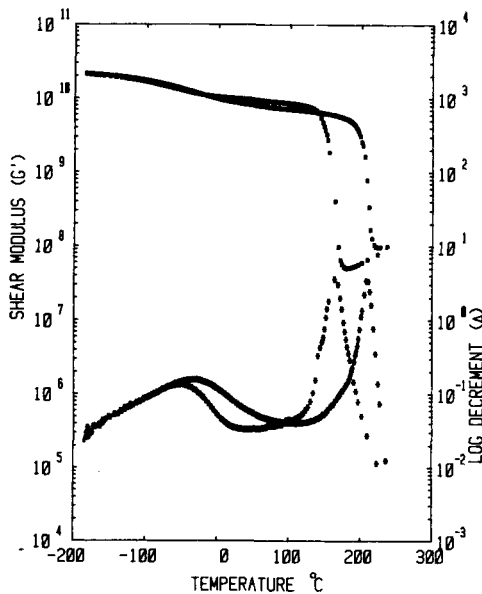
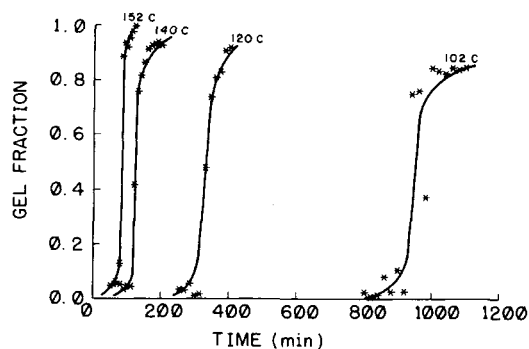
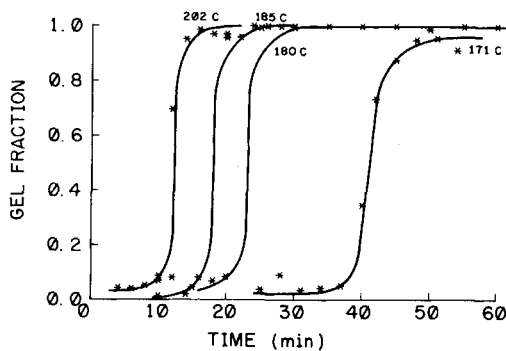


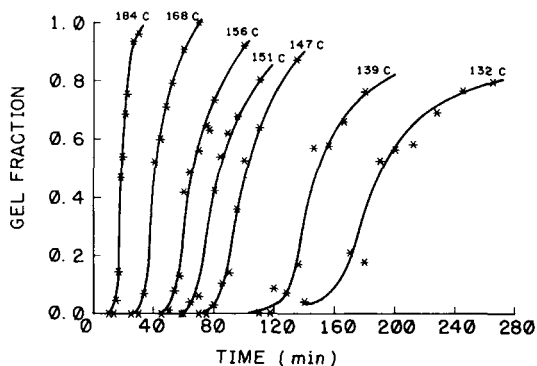
Fig. 7. Torsion pendulum spectra of film:  $-190^{\circ}\text{C}$  to  $250^{\circ}\text{C}$  (after partial cure at  $175^{\circ}\text{C}$ );  $250^{\circ}\text{C}$  to  $-190^{\circ}\text{C}$  (after full cure). The rate of change of temperature was  $\pm 1.5^{\circ}\text{C}/\text{min}$ .



(a)



(b)



(c)

Fig. 8. Gel fraction (Epon 828/DDS) vs. cure time at various temperatures: (a,b) in air; (c) in helium.

defined as the onset of insolubility, and calculated using the zero intercept of the extrapolated gel fraction curves, are tabulated in Table II.

**Water Absorption.** Films of Epon 828/DDS were prepared as described above for different times of cure at 175°C; i.e., 50, 100, 180, and 600 min. The specimens were prepared in order of diminishing cure time; the 600-min-cured specimens were prepared first, and the 50-min-cured specimens were cured last, so that changes due to physical aging would minimize rather than enhance dif-



TABLE II  
Gel Times from Gel Fraction Experiments

Temp (°C)	Gel time (min)	
	Air	Helium
202	9	
185	15	15
180	18	
173	30	
171	38	
168		32
165	48	
156		49
152	73	
151		62
147		77
140	110	
139		120
132		135
120	315	
102	920	

ferences in density between the specimens.<sup>5</sup> After the specimens had been stored in a vacuum oven at 50°C for 2 days, three specimens of each degree of cure were exposed to each of four different relative humidity atmospheres, 31%, 51%, 79.3%, and 93%, generated by saturated solutions of calcium chloride hexahydrate, calcium nitrate, ammonium chloride, and ammonium dihydrogen phosphate, respectively, at  $25 \pm 0.5^\circ\text{C}$ . Each film was suspended by a hook over a saturated salt solution in a sealed test tube. The moisture uptake was measured by intermittently removing the films from the test tubes and weighing them on a microbalance. The average percent weight gain of three specimens is plotted vs.  $(\text{time})^{1/2}$  in Figures 9–12 for each of the relative humidities to which they were

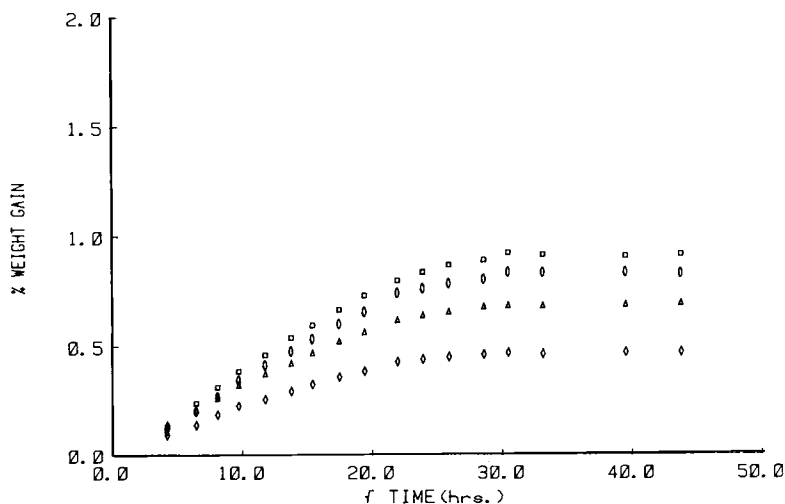


Fig. 9. Water absorption vs.  $\text{time}^{1/2}$  at 31% relative humidity. Cure time at  $175^\circ\text{C}$ : (◇) 50 min; (△) 100 min; (□) 180 min; (○) 600 min.

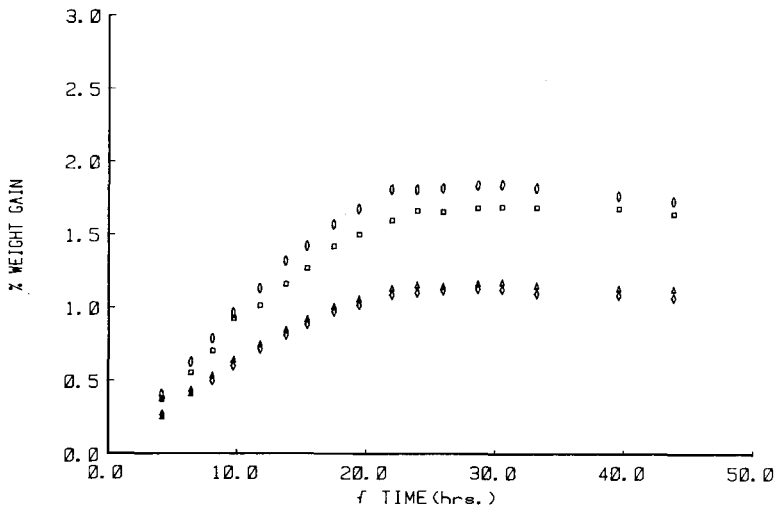


Fig. 10. Water absorption vs.  $\text{time}^{1/2}$  at 51% relative humidity (see caption for Fig. 9).

exposed. [A more rigorous approach would have involved plotting % weight gain vs.  $(\text{time})^{1/2}/\text{thickness}$ .]

After 2000 h of exposure, the samples were dried in a vacuum oven at  $50^\circ\text{C}$  for 2 weeks; their weights came to within  $0.028\% \pm 0.060$  of the initial weights.

**Density.** Densities of the cured epoxy specimens were measured in a density gradient column (ASTM D1505) at  $25^\circ\text{C}$ , prepared from mixtures of *o*-dichlorobenzene and toluene, which had been calibrated with calibration floats with densities 1.2320, 1.2344, and 1.2379 g/mL. Densities of specimens were determined by interpolating the calibration curve at the levels at which they came to rest (Fig. 13). Measurements were made 1 h after lowering the specimens into the column since their positions drifted over the course of several days due to swelling.

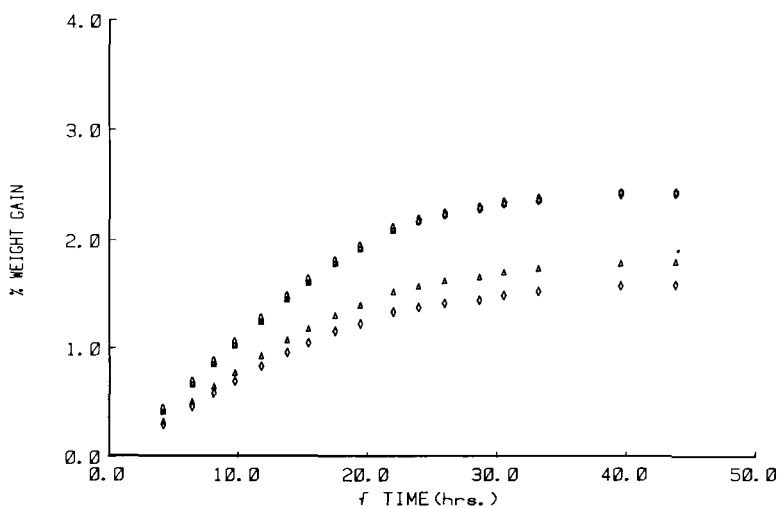


Fig. 11. Water absorption vs.  $\text{time}^{1/2}$  at 79.3% relative humidity (see caption for Fig. 9).

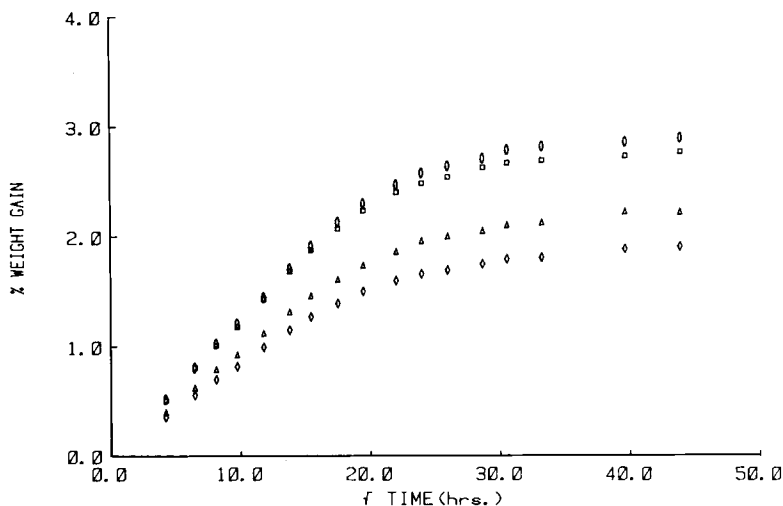


Fig. 12. Water absorption vs. time<sup>1/2</sup> at 93% relative humidity (see caption for Fig. 9).

## RESULTS AND DISCUSSION

A TTT diagram for Epon 828/DDS was constructed (Fig. 14) using the information obtained from the TBA and gel fraction experiments. A comparison of the gel fraction data with the TBA liquid-to-rubber transformation in a  $\ln(\text{time})$  vs.  $1/T$  plot (Fig. 15) indicates that there is a direct correlation between gelation and the liquid-to-rubber transformation. This relationship was also observed in the Epon 825/DDS and Epon 834/DDS systems,<sup>3,8</sup> whereas the correlation is not as good for the Epon 828/PACM-20 system.<sup>3</sup> Only the top portion (above 80°C) of the TTT diagram for Epon 828/DDS (Fig. 14) was obtained, since the presence of the solvent might have affected the TBA spectrum (bp MEK = 79°C). Using the TTT diagram and the  $T_g$  vs.  $T_{\text{cure}}$  plot (Fig. 4), a cure temperature could be chosen (175°C) at which the glass transition of the cured resin should eventually approach  $T_{g\infty}$  (Fig. 6). A reason for using one cure

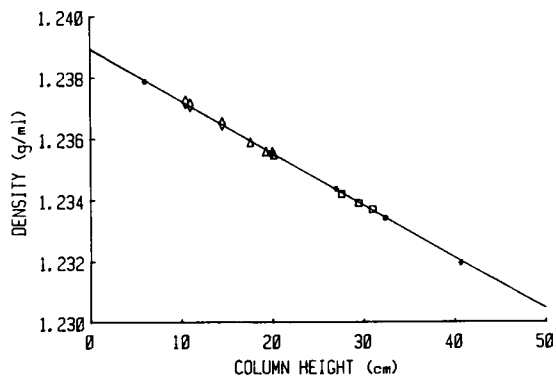


Fig. 13. Density gradient column data: (\*) calibrated floats. Specimens cured at 175°C: (◇) 50 min; (△) 100 min; (□) 180 min; (○) 600 min.

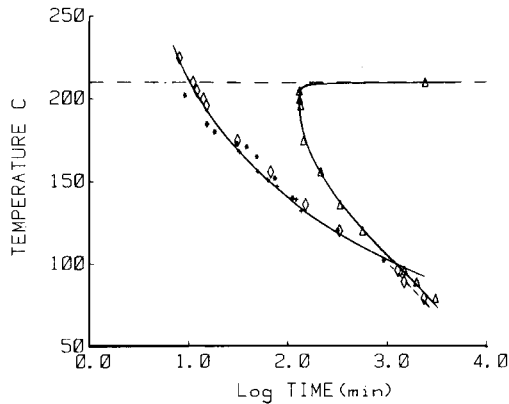


Fig. 14. TTT cure diagram. The maximum temperature ( $T_{g\infty}$ ) above which vitrification will not occur on isothermal cure is shown as a horizontal dashed line. The temperature of 175°C was selected for preparation of specimens with different extents of cure. (O) Liquid-to-rubber (TBA); ( $\Delta$ ) vitrification (TBA); (\*) gelation (gel fraction: air); (+) gelation (gel fraction: helium).

temperature to study the effect of the extent of cure on the physical properties is to eliminate the effect of other factors. For example, the reaction mechanism might be temperature-dependent, or the fractional free volume locked into the crosslinked network may be a function of the cure temperature.<sup>9</sup>

Although the equilibrium modulus might be expected to increase with increasing crosslink density, the modulus between  $T_{sec}$  and  $T_g$  (Fig. 7) of the fully cured film is lower than that of the partially cured film. This apparently anomalous result will be discussed later in the light of the other results.

The absorption of water by an epoxy film has been considered to occur by simple Fickian diffusion. The moisture concentration in a thin film at constant

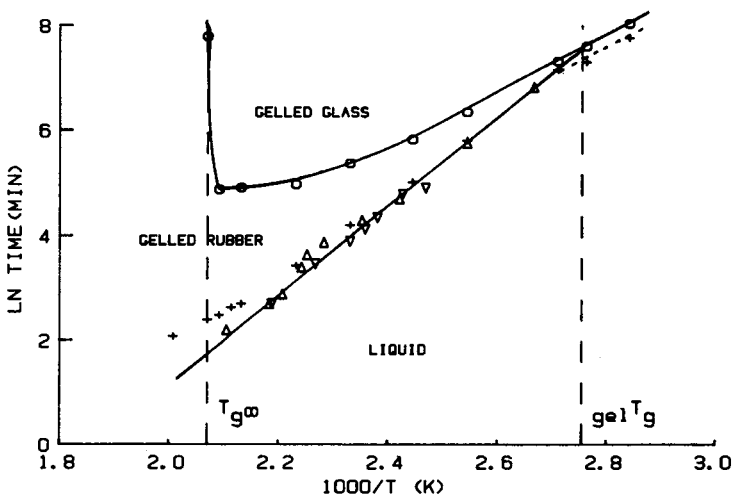


Fig. 15. Arrhenius plot of gel points and TBA data: ( $\Delta$ ) gel fraction (in air); ( $\nabla$ ) gel fraction (in helium); (+) liquid-to-rubber transformation (TBA); (O) vitrification (TBA).

temperature can be described by Fick's second law for 1-dimensional diffusion:

$$\frac{\partial c}{\partial t} = D_x \frac{\partial^2 c}{\partial x^2} \quad (1)$$

where  $c$  is the moisture concentration at time  $t$ ,  $D_x$  is the diffusivity of the penetrant in the direction normal to the surface, and  $x$  is the distance into the film from the surface. On solving eq. (1) and integrating over the film thickness,<sup>10</sup> the percent moisture content  $M$  (% weight gain) of the material as a function of time is

$$M = G(M_\infty - M_0) + M_0 \quad (2)$$

where  $M_0$  is the initial moisture content,  $M_\infty$  is the equilibrium moisture content, and  $G$  is a time-dependent parameter

$$G = 1 - \frac{8}{\pi^2} \sum_{i=0}^{\infty} \exp \frac{[-(2i+1)^2 \pi^2 D_x t / h^2]}{(2i+1)^2} \quad (3)$$

which can be approximated<sup>11</sup> by

$$G = 1 - \exp[-7.3(D_x t / h^2)^{0.75}] \quad (4)$$

where  $h$  is the film thickness.

The diffusivity  $D$  is obtained from the initial slope of the  $M$  vs.  $\sqrt{t}$  curve

$$D = \pi \left( \frac{h}{4M_\infty} \right)^2 \left( \frac{M_2 - M_1}{\sqrt{t_2} - \sqrt{t_1}} \right)^2 \quad (5)$$

and, if the moisture entering the specimen through the edges is considered,

$$D_x = \frac{D}{(1 + h/l + h/w)^2} \quad (6)$$

where  $l$  is the length and  $w$  is the width of the specimen.<sup>11</sup>

The equilibrium moisture content is a function of the relative humidity  $\phi$  of the air to which it is exposed<sup>12</sup>:

$$M_\infty = a\phi^b \quad (7)$$

The constants  $a$  (absorptivity) and  $b$  are selected to provide the best fit to the data.

The equilibrium moisture level  $M_\infty$  and diffusivity  $D_x$  of the films at each of the extents of cure and relative humidity can be obtained directly from Figures 9–12 and are tabulated in Table III. Although there was considerable scatter in the equilibrium moisture content of specimens that had the same cure history and relative humidity exposure, the trends were the same for each of the levels of relative humidity, with one exception [the film cured for 180 min had a higher equilibrium moisture content than the film cured for 600 min after exposure to 31% relative humidity (Fig. 9)]. In general, the films that were cured to a greater extent showed a higher equilibrium moisture content.

The diffusivity data show even greater scatter, and thereby perhaps provide a clue to some of the problems inherent in the experiment. Although the diffusivity is expected to remain constant with respect to relative humidity, it varies

TABLE III  
Density,  $T_g$ , Diffusivity, Absorptivity, and Equilibrium Moisture Content as a Function of Cure

Cure time at 175°C (min)	$T_g$ (°C)	Density (g/mL) at 25°C	Absorptivity ( $\times 10^2$ ) at 25°C	Relative humidity				
				31%	51%	79.3%	93%	
50	135	1.2370	2.2340	$M_\infty^a$	0.474	1.074	1.584	1.908
				$D_x^b$	1.2656	1.6900	1.1587	1.1868
100	160	1.2357	2.4368	$M_\infty$	0.696	1.136	1.803	2.224
				$D_x$	1.1718	1.7707	1.1984	1.1894
180	185	1.2339	2.9618	$M_\infty$	0.918	1.650	2.429	2.771
				$D_x$	1.2932	1.5885	1.2291	1.2360
600	195	1.2334	3.1933	$M_\infty$	0.831	1.737	2.426	2.897
				$D_x$	1.4094	1.7170	1.1705	1.2127

<sup>a</sup>  $M_\infty$  = moisture/(dry weight)  $\times 100$  at 25°C.

<sup>b</sup>  $D_x$  (cm<sup>2</sup>/s)  $\times 10^{-9}$  at 25°C.

as much with relative humidity as it does with extent of cure. Unusually high values were observed for 51% relative humidity, which is an indication that something unanticipated occurred with that set of specimens.

The equilibrium moisture content of the films cured to different extents is plotted vs. relative humidity in Figure 16. Since  $b$  [in eq. (7)] is equal to 1, the slopes provide the absorptivities ( $a$ ) which are seen to increase with increasing extent of cure. Both the higher equilibrium moisture content and higher absorptivity with increasing cure suggest increasing free volume, and hence an increasing specific volume with increasing cure. This is borne out by the density measurements, which indicate that the room temperature density decreases with increasing cure. Although this is in agreement with the work of Shimazaki,<sup>13</sup> it runs contrary to conventional wisdom.<sup>14,15</sup> A linear plot of absorptivity vs. specific volume (Fig. 17) suggests that a linear relationship exists between absorptivity and free volume  $V$ :

$$a = KV$$

where  $K = 4.05 \times 10^{-2}$  g/mL.

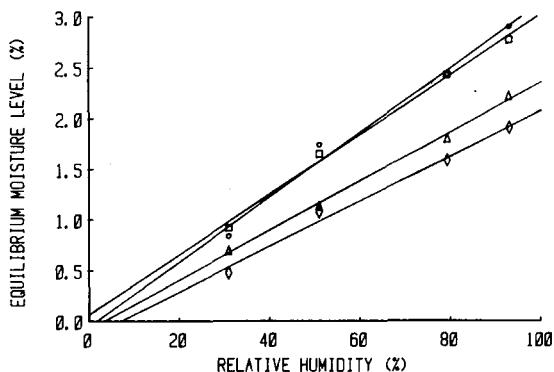


Fig. 16. Equilibrium moisture content vs. relative humidity. Specimens cured at 175°C for: ( $\diamond$ ) 50 min; ( $\Delta$ ) 100 min; ( $\square$ ) 180 min; ( $\circ$ ) 600 min.

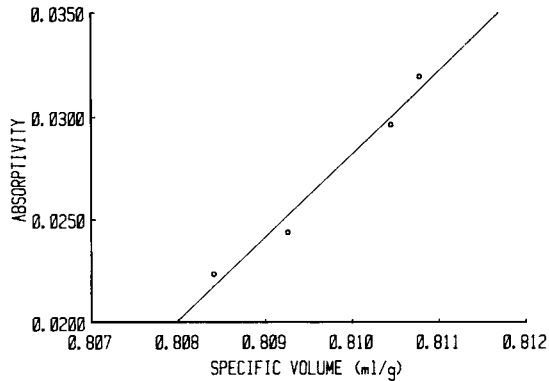


Fig. 17. Absorptivity vs. specific volume.

The key to understanding this apparently anomalous behavior is to note that the temperature at which the density and water absorption were measured (25°C) was below the glass transition temperature. Schematic plots of specific volume versus temperature for a partially cured and fully cured material are shown in Figure 18. In the rubbery state above  $T_{g\infty}$ , the density of the more highly crosslinked material is higher; but its  $T_g$  is also higher, and as a result the specific volume versus temperature curves can cross,<sup>1,13</sup> resulting in a lower density at room temperature for the more highly crosslinked material. The lower room temperature modulus<sup>6,16</sup> for a more highly crosslinked material can now be understood as well, since it is directly proportional to density.

This dependence of specific volume at room temperature on the glass transition has also been observed in amorphous linear polymers. Ueberreiter and Kanig<sup>17</sup> demonstrated that the room temperature density of polystyrene decreased as its molecular weight (and  $T_g$ ) increased.

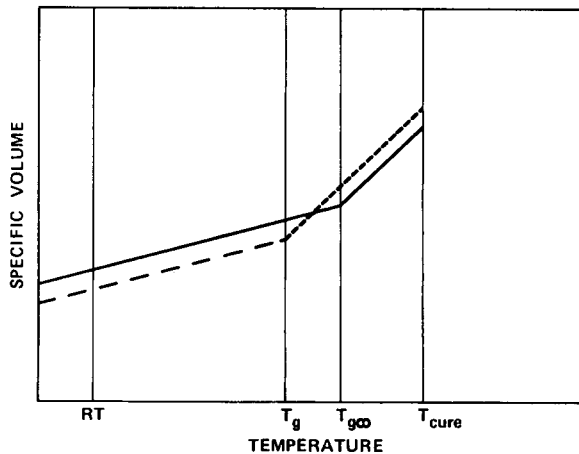


Fig. 18. Volume-temperature plots of a thermoset with two levels of crosslink density (schematic) in the absence of further reaction during the temperature scan.

## CONCLUSIONS

These experiments on epoxy resins have shown that the lower modulus and higher equilibrium moisture content of the more highly cured resins at room temperature are a consequence of the lower density which in turn is a result of the increase in  $T_g$  as a function of cure. At room temperature the more highly cured material is further from equilibrium, and therefore has more free volume than a material cured to a lesser extent.

Partial financial support was provided by the Chemistry Branch of the office of Naval Research.

## References

1. J. K. Gillham, in *Developments in Polymer Characterization-3*, J. V. Dawkins, Ed., Applied Science, London, 1982, pp. 159-227.
2. J. B. Enns and J. K. Gillham, in *Computer Applications in Applied Polymer Science*, T. Provder, Ed., ACS Symposium Series, No. 197, American Chemical Society, Washington, D.C., 1982, pp. 329-352.
3. J. B. Enns and J. K. Gillham, *J. Appl. Polym. Sci.*, **28**, 2567 (1983).
4. J. B. Enns and J. K. Gillham, in *Polymer Characterization: Spectroscopic, Chromatographic, and Physical Instrumental Methods*, C. D. Craver, Ed., Advances in Chemistry Series, No. 203, American Chemical Society, Washington, D.C., 1983, pp. 27-63.
5. J. P. Aherne, J. B. Enns, M. J. Doyle, and J. K. Gillham, *Am. Chem. Soc., Div. Org. Coat. Plast. Chem., Prepr.*, **46**, 574 (1982).
6. G. A. Pogany, *Polymer*, **11**, 66 (1970).
7. N. S. Schneider and J. K. Gillham, *Polym. Compos.*, **1**, 97 (1980).
8. J. B. Enns, Ph.D. thesis, Princeton University, 1982.
9. M. B. Roller, *J. Coat. Technol.*, **54**, 33 (1982).
10. W. Jost, *Diffusion in Solids, Liquids, Gases*, Academic, New York, 1960.
11. C. H. Shen and G. S. Springer, *J. Compos. Mater.*, **10**, 2 (1976).
12. J. F. Carpenter, "Moisture Sensitivity of Epoxy Composites and Structural Adhesives," McDonnell Aircraft Co., Report MDC A2640, December 1973.
13. A. Shimazaki, *J. Polym. Sci., Part C*, **23**, 555 (1968).
14. L. E. Nielsen, *J. Macromol. Sci.*, **C3**, 69 (1969).
15. F. W. Billmeyer, *Textbook of Polymer Science*, Wiley-Interscience, New York, 1968, p. 231.
16. R. G. C. Arridge, and J. H. Speake, *Polymer*, **13**, 443 (1972).
17. K. Ueberreiter and G. J. Kanig, *J. Colloid Sci.* **7**, 569 (1953).

Received May 25, 1982

Accepted March 28, 1983